# A New Nodal Integration Method for Helmholtz Problems Based on Domain Decomposition Techniques

Martin J. Gander and Niteen Kumar

## 1 Introduction

Wave field simulations have many applications, from seismology over radiation to acoustics. The Helmholtz equation is used to model many of these phenomena, and several numerical schemes were developed for this, see e.g. [5, 8, 7] and references therein. However, to capture the accurate wave behavior, in general these schemes need very fine meshes, because of the so called pollution effect, see [1]. The fine mesh requirement results in large system matrices with bad condition number, and thus requires a huge computational effort, since Helmholtz problems are notoriously difficult to solve using iterative methods [4]. Also, due to the high condition number, often these schemes have numerical problems for large wave numbers.

We present in this short note a new Nodal Integration Method (NIM) based on domain decomposition techniques for the Helmholtz equation

$$\nabla^2 u(\mathbf{x}) + k^2 u(\mathbf{x}) = f(\mathbf{x}), \tag{1}$$

where $\mathbf{x}$ is the spatial position, $k$ is the wave number, $u$ represents the wave field, typically a pressure perturbation, and $f$ is the source term. NIM is a coarse mesh numerical scheme based on the transverse integration process (TIP) and analytical solutions of the ODEs resulting from TIP [10]. NIM has an edge over other schemes due to the inbuilt semi-analytical approach in the scheme development process, which closely relates the scheme to the physical problem compared to predefined basis-function based methods such as finite-element methods. NIM schemes are related to Trefftz methods [12] going back to Erich Trefftz in 1926 as a counterpart of the classical Ritz method [11] from 1909. Trefftz methods use basis functions that satisfy the homogeneous equations exactly within elements, see also [8] and references therein, whereas NIMs satisfy only one dimensional averaged equations.

Martin J. Gander, Niteen Kumar
Section de Mathématiques, Université de Genève, e-mail: martin.gander@unige.ch, niteen.kumar@unige.ch

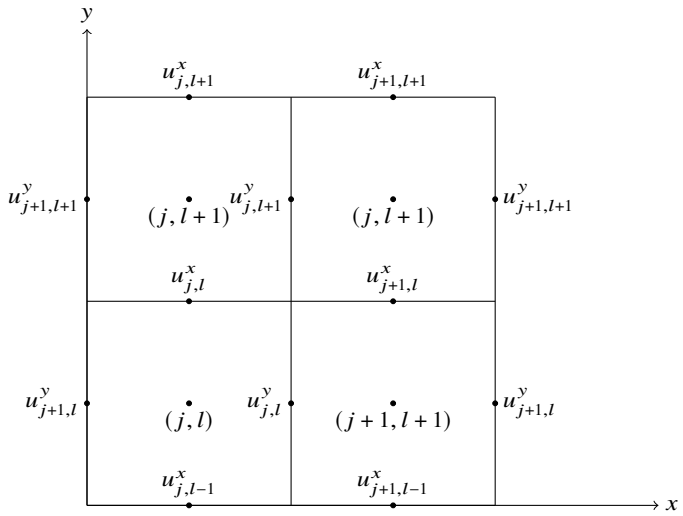


**Fig. 1** Arrangement of elements in 2D called nodes in NIM.

The first NIM scheme was developed for simulations in nuclear industry [6], and NIM found its acceptance in other engineering domains as well, due to high accuracy with coarser meshes, see e.g. [9] and references therein. The discretization of PDEs is also often plagued with numerical dispersion, and NIM schemes show minimal dispersion compared to other schemes, see [10], and [2] and references therein for more information about dispersion correction. We propose here a new NIM scheme for the Helmholtz equation to improve the conditioning of the resulting system matrix, and further reduce dispersion. Our new approach uses impedance (or Robin) conditions in its construction, in contrast to the classical Dirichlet and Neumann conditions in earlier NIMs for Helmholtz problems.

## 2 Classical NIM for the Helmholtz problem

In order to derive the classical NIM scheme for the Helmholtz equation (1) in 2D, the domain is divided into $n$ rectangular elements of size $h$ called nodes, see Figure 1. For each node, a local coordinate system is defined with its origin at the node center. The Helmholtz Equation (1) can be written with reference to node $(j, l)$ as

$$\nabla^2 u_{j,l}(x, y) + k^2 u_{j,l}(x, y) = f_{j,l}(x, y), \quad (x, y) \in \Big( -\frac{h}{2}, \frac{h}{2}) \Big) \times \Big( -\frac{h}{2}, \frac{h}{2} \Big). \quad (2)$$

In NIM, the PDE is first averaged within a node to remove the dependency in one spatial directions, which results in an approximate ODE. This is called the transverse integration process (TIP). To perform the TIP, Equation (2) is averaged using the

operator $\frac{1}{h}\int_{-h/2}^{+h/2} \mathrm{d}x$ in x-direction and the operator $\frac{1}{h}\int_{-h/2}^{+h/2} \mathrm{d}y$ in y-direction. On performing the TIP (averaging) for example in the $x$-direction,

$$\frac{1}{h}\int_{-h/2}^{+h/2}\left(\frac{\mathrm{d}^2 u_{j,l}(x,y)}{\mathrm{d}x^2}+\frac{\mathrm{d}^2 u_{j,l}(x,y)}{\mathrm{d}y^2}+k^2 u_{j,l}(x,y)=f_{j,l}(x,y)\right)\mathrm{d}x, \tag{3}$$

we get x-averaged ODEs whose solutions are a function of $y$ only as given in equation (4) below. Similarly, performing TIP on equation (2) in the $y$-direction gives us y-averaged ODEs whose solutions are a function of $x$ only,

$$\frac{\mathrm{d}^2 \overline{u}^x_{j,l}(y)}{\mathrm{d}y^2}+k^2\overline{u}^x_{j,l}(y)=\overline{S}^x_{j,l}(y), \quad \frac{\mathrm{d}^2 \overline{u}^y_{j,l}(x)}{\mathrm{d}x^2}+k^2\overline{u}^y_{j,l}(x)=\overline{S}^y_{j,l}(x). \tag{4}$$

Here the solution variables represent averaged quantities,

$$\overline{u}^x_{j,l}(y):=\frac{1}{h}\int_{-h/2}^{+h/2} u_{j,l}(x,y)\mathrm{d}x, \quad \overline{u}^y_{j,l}(x):=\frac{1}{h}\int_{-h/2}^{+h/2} u_{j,l}(x,y)\mathrm{d}y, \tag{5}$$

and also the source term $f_{j,l}$ was averaged including the remaining transverse term,

$$\overline{S}^x_{j,l}(y):=\frac{1}{h}\int_{-h/2}^{+h/2}\left(f_{j,l}(x,y)-\frac{\partial^2 u_{j,l}(x,y)}{\partial x^2}\right)\mathrm{d}x, \tag{6}$$

$$\overline{S}^y_{j,l}(x):=\frac{1}{h}\int_{-h/2}^{+h/2}\left(f_{j,l}(x,y)-\frac{\partial^2 u_{j,l}(x,y)}{\partial y^2}\right)\mathrm{d}y. \tag{7}$$

After the TIP, the set of approximate ODEs given in Equation (4) is solved analytically within two consecutive nodes, using an appropriate approximation of the source term to make this analytical integration possible (for example a truncated Legendre expansion). After the integration, the two analytical solutions are connected using coupling conditions, classically Dirichlet continuity is imposed by imposing a common (unknown) value, which is then determined imposing Neumann continuity, like in a substructuring domain decomposition method. This results in two three point schemes, one in the $x$-direction and the other in the $y$-direction. From these three point schemes, the pseudo source is finally eliminated using constraint conditions, which results in the final set of algebraic equation for the scheme, see [6, 9, 10] for more details, and below for a simple example.

While this NIM scheme for Helmholtz is working, the resulting matrix elements can have a strong dependence on the wave number $k$. We show in Table 1 an example of the dependence of the system matrix norm on the wave number $k$ of the 2D NIM scheme described above. This strong dependence is numerically not desirable, especially when the mesh resolution is not changed as in our example, there is too much sensitivity with respect to the wave number in this discrete problem.

In order to better understand this strong dependence on the wave number $k$ of the classical NIM system matrix for the Helmholtz equation, we now study in more detail the one dimensional case,

**Table 1** Dependence of the system matrix norm on the wave number $k$ for the classical NIM scheme in 2D for the Helmholtz equation.

| Wave number ($k$) | NIM matrix norm (2D-Helmholtz) |
|---|---|
| 150 | 14800 |
| 151 | 32170 |
| 152 | 214350 |
| 153 | 25180 |
| 154 | 13500 |

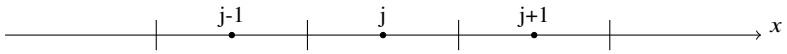


**Fig. 2** Arrangement of elements in 1D.

$$\partial_{xx} u_j(x) + k^2 u_j(x) = f_j(x), \quad x \in \Big(-\frac{h}{2}, \frac{h}{2}\Big), \tag{8}$$

see also Figure 2. In one dimension, the TIP is not necessary, except for the right hand side function $f_j(x)$. Here we expand $f_j(x)$ in Legendre polynomials and truncate to the first term, i.e. the constant, which we call $S_j$. This approximation to a constant term leads to second order accuracy in the scheme. We can then directly solve Equation (8) analytically with $f_j(x)$ replaced by $S_j$ on each node, and using Dirichlet boundary conditions, which are

$$\left.\begin{aligned} \overline{u}^a_j(x)\Big|_{-h/2} &= u_{j-1} \\ \overline{u}^a_j(x)\Big|_{h/2} &= u_j \end{aligned}\right\} \text{for node } j, \qquad \left.\begin{aligned} \overline{u}^a_{j+1}(x)\Big|_{-h/2} &= u_j \\ \overline{u}^a_{j+1}(x)\Big|_{h/2} &= u_{j+1} \end{aligned}\right\} \text{for node } j+1. \tag{9}$$

The analytical solution for node $j$ and $j+1$ is then given by

$$\begin{aligned} \overline{u}^a_j(x) &= \tfrac{2S_j + (-2S_j + k^2(u_j + u_{j-1}))\cos kx \sec\frac{hk}{2} + k^2(u_j - u_{j-1})\csc\frac{hk}{2}\sin kx}{2k^2}, \\ \overline{u}^a_{j+1}(x) &= \tfrac{2S_{j+1} + (-2S_{j+1} + k^2(u_j + u_{j+1}))\cos kx \sec\frac{hk}{2} + k^2(u_{j+1} - u_j)\csc\frac{hk}{2}\sin kx}{2k^2}. \end{aligned} \tag{10}$$

Now in order to connect consecutive nodes, the matching of Neumann traces is imposed, i.e.

$$\left(\frac{d\overline{u}^a_j(x)}{dx}\right)\Big|_{h/2} = \left(\frac{d\overline{u}^a_{j+1}(x)}{dx}\right)\Big|_{-h/2}. \tag{11}$$

This leads to a finite difference like stencil for the unknown Dirichlet values $u_j$, which contains in its coefficients information about the physical problem that is solved, namely

$$\frac{k}{\sin kh} u_{j+1} - \frac{2k}{\tan kh} u_j + \frac{k}{\sin kh} u_{j-1} = \frac{\tan\frac{hK}{2}}{k}(S_j + S_{j+1}). \tag{12}$$

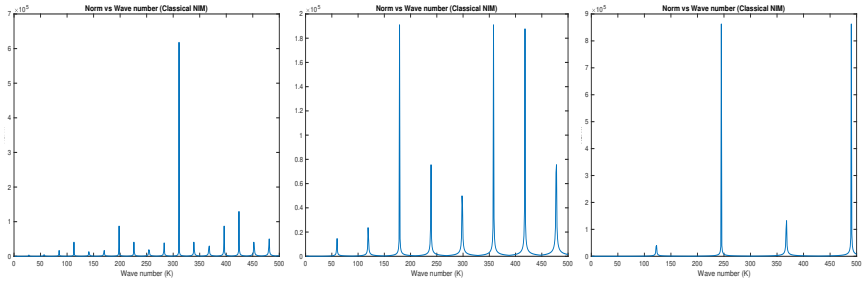


**Fig. 3** Norms of the system matrix of the classical Helmholtz NIM from the stencils (12), (14), (15) for varying wave number $k$ and three mesh sizes: 0.1 (left), 0.05 (middle) and 0.025 (right).

To complete the linear system, we have to use on the first node, $j = 1$, and the last node, $j = J$, the original boundary conditions imposed on the problem, which we assume to be of impedance type,

$$\left(-\frac{d\overline{u}_1^a(x)}{dx} + ik\overline{u}_1^a(x)\right)\Bigg|_{-h/2} = 0, \quad \left(\frac{d\overline{u}_J^a(x)}{dx} + ik\overline{u}_J^a(x)\right)\Bigg|_{h/2} = 0. \tag{13}$$

This leads for the first and last NIM matrix equations to the stencils

$$\left(\frac{ik + k^2 \cot hk}{k}\right) u_1 - (k \csc hk) u_2 = \left(\frac{\cot hk - \csc hk}{k}\right) S_2, \tag{14}$$

$$\left(\frac{ik + k^2 \cot hk}{k}\right) u_J - (k \csc hk) u_{J-1} = \left(\frac{\cot hk - \csc hk}{k}\right) S_J. \tag{15}$$

Collecting these stencils in the associated system matrix of the Helmholtz NIM in 1D, and computing its norm, we find the results shown in Figure 3. Clearly the norm is extremely sensitive to the wave number $k$, and this does not improve when the mesh is refined. We can now also see the reason for this looking at the stencil entries: in the interior stencil in (12), the stencil coefficients contain a division by $\sin kh$, and this quantity becomes zero for $k = \ell\pi/h$, $\ell = 1, 2, \ldots$, which explains the poles in Figure 3 and more generally the sensitivity of the classical Helmholtz NIM matrix norm on the wave number. We can now also explain the reason for this sensitivity: in the construction of the classical Helmholtz NIM, we solved 1D Helmholtz problems on each node, imposing Dirichlet boundary conditions, and if $k^2$ corresponds to an eigenvalue of the one dimensional Laplacian, then this problem is not well posed, a fact that manifests itself in the division by zero in the stencil coefficients.

## 3 Derivation of the new NIM scheme

To address the issue of division by zero for some values of $k$, we must design a new Helmholtz NIM that avoids in its construction the solution of Helmholtz problems with Dirichlet conditions that can become ill-posed. This can be achieved by using impedance conditions instead, like it was proposed in the seminal work of Després and his non-overlapping Schwarz method for Helmholtz problems [3]. We thus replace in the construction of our new Helmholtz NIM the conditions (9) for nodes $j$ and $j+1$ by the conditions

$$\left.\begin{aligned} &\left(-\frac{\partial \overline{u}_j^a(x)}{\partial x} + ik\overline{u}_j^a(x)\right)\Big|_{-h/2} = \sigma_{j-1} \\ &\left(\frac{\partial \overline{u}_j^a(x)}{\partial x} + ik\overline{u}_j^a(x)\right)\Big|_{h/2} = \lambda_j \end{aligned}\right\} \text{for node } j, \tag{16}$$

$$\left.\begin{aligned} &\left(-\frac{\partial \overline{u}_{j+1}^a(x)}{\partial x} + ik\overline{u}_{j+1}^a(x)\right)\Big|_{-h/2} = \sigma_j \\ &\left(\frac{\partial \overline{u}_{j+1}^a(x)}{\partial x} + ik\overline{u}_{j+1}^a(x)\right)\Big|_{h/2} = \lambda_{j+1} \end{aligned}\right\} \text{for node } j+1. \tag{17}$$

Instead of the unknown Dirichlet values $u_j$ in the original Helmholtz NIM, now the unknowns are the impedance traces $\lambda_j$ and $\sigma_j$, which means that we construct directly a right preconditioned system in this new Helmholtz NIM design. The analytical solution of the Helmholtz equation (8) with constant source term $S_j$ and node impedance boundary conditions (16) on node $j$ is

$$\overline{u}_j^a(x) = \frac{2S_j + e^{\frac{-ik(h+2x)}{2}}(-S_j - e^{2ikx}(S_j + ik\lambda_j) - ik\sigma_j}{2k^2}, \tag{18}$$

and similarly we find on node $j+1$

$$\overline{u}_{j+1}^a(x) = \frac{2S_{j+1} + e^{\frac{-ik(h+2x)}{2}}(-S_{j+1} - e^{2ikx}(S_{j+1} + ik\lambda_{j+1}) - ik\sigma_{j+1}}{2k^2}. \tag{19}$$

In order to obtain the new Helmholtz NIM scheme, we use impedance condition matching at the interface,

$$\sigma_{j+1} = \left(-\frac{d\overline{u}_j^a(x)}{dx} + ik\overline{u}_j^a(x)\right)\Big|_{h/2}, \quad \lambda_j = \left(\frac{d\overline{u}_j^a(x)}{dx} + ik\overline{u}_j^a(x)\right)\Big|_{-h/2}. \tag{20}$$

This leads to the new finite difference type stencil

$$\sigma_{j+1} - e^{-ihk}\sigma_j = \left(-\frac{i}{k} + \frac{ie^{-ikh}}{k}\right)S_j, \quad \lambda_j - e^{-ihk}\lambda_{j+1} = \left(-\frac{i}{k} + \frac{ie^{-ikh}}{k}\right)S_{j+1}. \tag{21}$$

For the first and last equation in the system, we need to use again the original boundary conditions in (13), which leads for $j = 1$ to

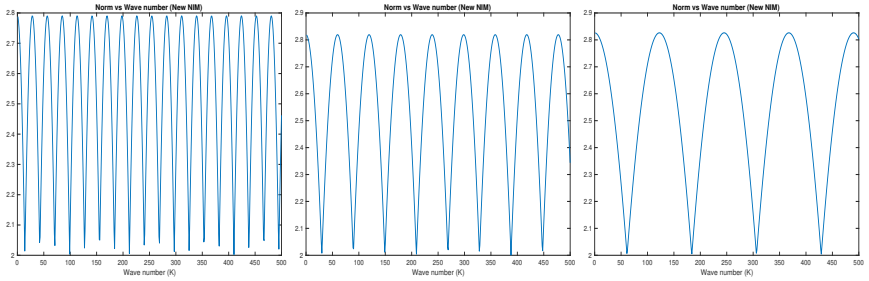


**Fig. 4** Norms of the system matrix of the new Helmholtz NIM from the stencils (21), (22), (23), for varying wave number $k$ and three mesh sizes: 0.1 (left), 0.05 (middle) and 0.025 (right).

$$\left(\frac{e^{ihk}(k-1)}{2k}\right)\lambda_1 + \left(\frac{k+1}{2k}\right)\sigma_1 = \left(\frac{-i(k-1)+ie^{ihk}(k-1)}{2k^2}\right)S_1. \tag{22}$$

Similarly the equation on the right boundary, $j = J$, is

$$-\left(\frac{e^{-ihk}(k-1)}{2k}\right)\sigma_J + \left(\frac{k+1}{2k}\right)\lambda_J = \left(\frac{-i(k-1)+ie^{-ihk}(k-1)}{2k^2}\right)S_J. \tag{23}$$

Now we can see from the stencil coefficients in Equation (21) of the new Helmholtz NIM that there is no singularity present any more, and thus the system matrix norms should not have this sensitive dependence on the wave number $k$ any longer. This is confirmed in Figure 4, where we plot the system matrix norm of our new Helmholtz NIM for three different mesh sizes as a function of the wave number $k$. We see that the norm stays nicely bounded below 3, whereas for the classical NIM the matrix norms we observed were of the order of $1e5$.

## 4 Conclusions

We presented a new nodal integration method (NIM) based on domain decomposition techniques for the Helmholtz equation. In our new Helmholtz NIM, instead of Dirichlet and Neumann transmission conditions that are usually used in the construction of the NIM, we used impedance (or Robin) transmission conditions. This modification changes the coefficients as well as the resulting system matrix structure, and we observe that the new system matrix has nicely bounded norms for all wave numbers, while the original NIM system matrix norm presented singularities. However, the new system matrix is now twice the size of the old system matrix, since we are solving for the Robin traces as unknowns. We gain stability at the cost of a bigger system matrix. We are currently developing our new Helmholtz NIM in two and three spatial dimensions, and also investigate if it is possible to use impedance conditions without

increasing the system matrix size. We are also studying the dispersion relation properties of our new Helmholtz NIM, and investigate its potential for dispersion correction.

## References


1. Babuska, I. M. and Sauter, S. A. Is the pollution effect of the FEM avoidable for the Helmholtz equation considering high wave numbers? *SIAM Journal on numerical analysis* **34**(6), 2392–2423 (1997).
2. Cocquet, P.-H., Gander, M. J., and Xiang, X. Closed form dispersion corrections including a real shifted wavenumber for finite difference discretizations of 2d constant coefficient Helmholtz problems. *SIAM Journal on Scientific Computing* **43**(1), A278–A308 (2021).
3. Després, B. Décomposition de domaine et problème de Helmholtz. *C.R. Acad. Sci. Paris* **1**(6), 313–316 (1990).
4. Ernst, O. G. and Gander, M. J. Why it is difficult to solve Helmholtz problems with classical iterative methods. *Numerical analysis of multiscale problems* 325–363 (2012).
5. Feng, W. Discontinuous Galerkin methods for the Helmholtz equation with large wave number. *SIAM Journal of Numerical analysis* **47**(4), 1–10 (2009).
6. Ferrer, R. M. and Azmy, Y. Y. Error analysis of the nodal integral method for solving the neutron diffusion equation in two-dimensional cartesian geometry. *Nuclear Science and Engineering* **162**(3), 215–233 (2009).
7. Griesmaier, R. and Monk, P. Error analysis for a hybridizable discontinuous Galerkin method for the Helmholtz equation. *Journal of Scientific Computing* **40**(1), 291–310 (2011).
8. Hiptmair, R., Moiola, A., and Perugia, I. Trefftz discontinuous Galerkin methods for acoustic scattering on locally refined meshes. *Applied Numerical Mathematics* **79**(1), 79–91 (2014).
9. Kumar, N., Majumdar, R., and Singh, S. Predictor-Corrector Nodal Integral Method for simulation of high Reynolds number fluid flow using larger time steps in Burgers' equation. *Computers and Mathematics with Applications* **79**(5), 1362–1381 (2020).
10. Kumar, N., Shekar, B., and Singh, S. A nodal integral scheme for acoustic wavefield simulation. *Pure and applied geophysics* **179**(1), 3677–3691 (2022).
11. Ritz, W. Über eine neue Methode zur Lösung gewisser Variationsprobleme der mathematischen Physik. *Journal für die reine und angewandte Mathematik* **135**, 1–61 (1909).
12. Trefftz, E. Ein Gegenstück zum Ritzschen Verfahren. In: *Proc. 2nd Int. Cong. Appl. Mech. Zurich*, 131–137 (1926).